

Coupled ENSO instabilities derived with breeding

Ming Cai and Eugenia Kalnay

Department of Meteorology, University of Maryland, College Park, MD 20742

This paper reports the ENSO instability properties derived from breeding experiments made with NASA NSIPP coupled GCM model. Bred vectors, the difference between a breeding run and the control run, are the naturally growing instabilities upon the evolving flow and are strongly related to forecast errors.

A 50-year control integration and two 10-year breeding experiments have been carried out using the NSIPP coupled model (1.25 by 2/3°, 20 layers in the ocean and 3.75 by 3°, 17 levels in atmosphere). Each of the two breeding experiments consists of 120 monthly integrations obtained by running the same executable file used for the control run, but with the control run restart files (initial conditions) to which we added a bred perturbation. We use as rescaling norm the rms of the SST difference between the control and perturbation run averaged over the tropical Pacific basin (15S-15N and 120-270) is used to measure the perturbation size (denoted as S). The perturbation for each monthly integration has the same value of S equal to 0.085 °C, about 10% of the SST variability over that area. The only difference between the two breeding runs is in the initial perturbation, which is determined from the differences between two randomly selected sets of restart files. Although the initial perturbations for the two breeding runs are substantially different in the ocean and especially in the atmosphere, the bred vectors generated by the two breeding runs have similar growth rates and spatial structures, implying the breeding method is indeed capable of capturing the fastest growing modes associated with background ENSO events.

The primary objective for these breeding runs is to assess whether it is feasible to separate the ENSO related coupled variability from the weather modes and other short time scale oceanic instabilities using the breeding technique. The results obtained with the Zebiak-Cane model (Cai et al. 2002) provide us with general guidelines for judging if the bred vectors obtained with the NSIPP model are those associated with ENSO-related coupled instability. Figure 1 shows monthly amplification rates derived from the two breeding runs with a reference to the evolution of the background ENSO events. The amplification rate of the bred vectors tends to be larger few month prior to or after a major extreme (warm/cold) event, in a good agreement with the results found in ZC model. The amplification rate is about 3 times as large as that found in the ZC model. The Niño-3 index of the bred vectors tends to have large amplitudes either before or after a major event (not shown). This again is consistent with the findings of the ZC model. The SOI indices of the bred vectors show similar characteristics. Another feature is that the two breeding runs (BV1 and BV2) show virtually the same behavior, except that occasionally the sign of the bred vectors in the two breeding runs is opposite. This may be viewed as independent evidence showing the evolution of the bred vectors is strongly dictated by the background ENSO events. We have calculated three sets of regression maps against the Niño-3 index of the control run, and the Niño-3 index of the bred vectors derived from the BV1 and BV2 runs. As shown in Figure 2, there is some similarity between the regression maps of the tropical variables calculated from the control run and their counterparts from the breeding runs, although the latter tend to be narrower and have smaller scales, as in the ZC model. This suggests that dominant patterns captured in the breeding runs are ENSO-like perturbations at least within the tropical Pacific basin, as in the ZC model. Moreover, the similarity of the patterns derived from the two breeding runs suggests that despite the presence of large amplitude atmospheric noise, there is a still a single dominant ENSO instability, and that this leads to the robustness of the pattern captured by the bred vectors. The variability associated with the pattern shown in the regression maps explains more than 40% of total variability of the perturbation fields over the tropical Pacific basin in the breeding runs.

We have also calculated the regression maps of 500 hPa geopotential height of the control run and bred vectors derived from the two breeding runs (not shown). Again, we find that the regression maps of the BV1 and BV2 resemble each another. However, unlike the tropical response, the variability associated with the patterns only explains about 15% of the total perturbation variability over the globe in the breeding runs. Therefore, if we interpret the patterns shown in the regression maps to be associated with tropical ENSO variability, these signals are mixed with the background “weather noise” over the mid-latitudes. In other words, with the choice of ocean SST norm for rescaling, the breeding method is able to capture the ENSO-related instability over the tropical Pacific basin, but it cannot separate the remote

responses to the coupled tropical anomalies from the background weather noise over extratropics without using additional tools (such as the regression analysis). Since the breeding perturbations are associated with instabilities of the underlying flow and with forecast errors, we expect to be able to use these results within the data assimilation system and reduce the “errors of the month” within the analysis at low computational cost.

REFERENCES

Cai, M., E. Kalnay, and Z. Toth, 2002: Bred Vectors of the Zebiak-Cane Model and Their Application to ENSO Predictions. Accepted in J. Climate.

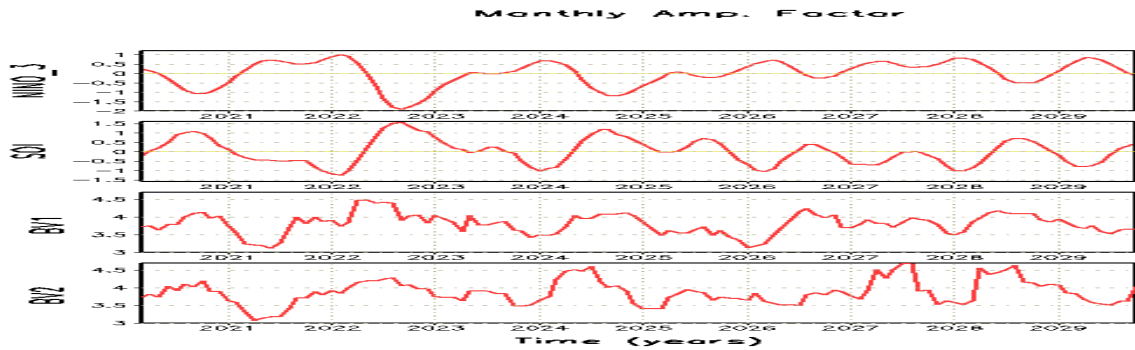


Figure 1. Monthly amplification factors of bred vectors of the NSIPP model. The top two panels are Niño-3 and SOI indexes of the background ENSO obtained from the control run. The bottom two panels are the monthly amplification factors of the two breeding runs.

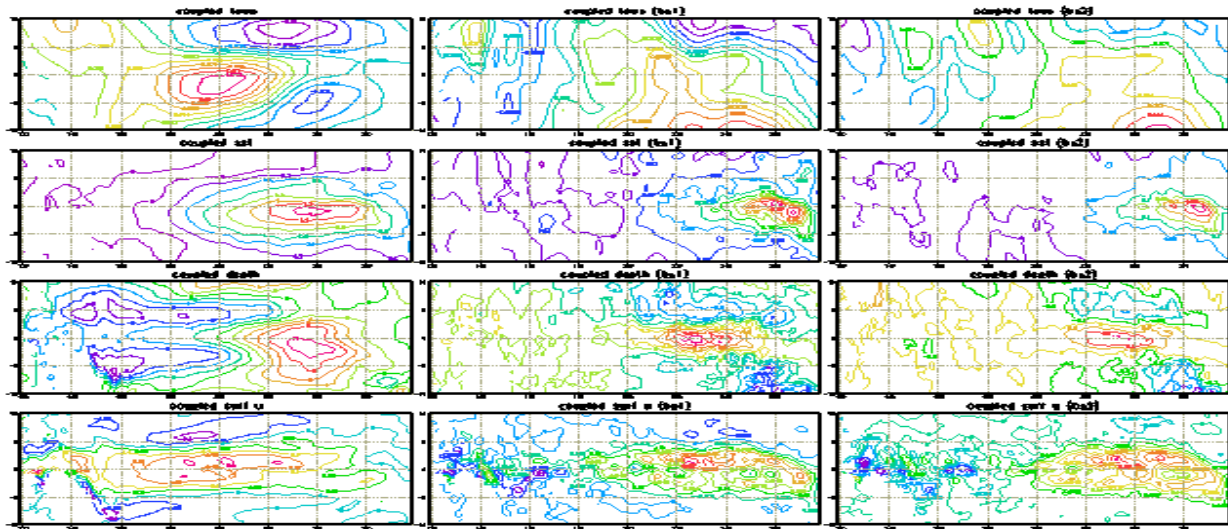


Figure 2. Regression maps of sample tropical variables (10S-10N) from the NSIPP model. The left panels are regression maps of the control run against the Niño-3 index of the control run, the middle panels are those of bred vectors derived from BV1 run against the Niño-3 index of the BV1 run, and the right panels are the same but for BV2. From the top to bottom, the variables are zonal wind stress, sea surface temperature, thermocline depth (the depth of the first seven layers), and surface zonal current.